Radiol med (2014) 119:842–851
DOI 10.1007/s11547-014-0398-8

PAEDIATRIC RADIOLOGY

Congenital cystic lung disease: prenatal ultrasound and postnatal multidetector computer tomography evaluation. Correlation with surgical and pathological data

Maria Pia Bondioni · Diego Gatta · Vassilios Lougaris · Nicoletta Palai · Marino Signorelli · Silvia Michelini · Giuseppe Di Gaetano · Paola Tessitore · Lorella Mascaro · Andrea Tironi · Giovanni Boroni · Roberto Maroldi · Daniele Alberti

Received: 16 October 2013 / Accepted: 22 November 2013 / Published online: 8 March 2014

Abstract
Purpose The aim of this study was to evaluate the diagnostic accuracy of postnatal multidetector computed tomography (MDCT) compared with prenatal ultrasound (US), surgical findings, and histology, in 33 patients with congenital cystic lung disease.
Methods Thirty-three patients, 17 males and 16 females, were evaluated by MDCT. Twenty-seven of these patients underwent prenatal US between week 18 and 22, and between week 32 and 35 of gestation. Lung lobectomy, segmentectomy, atypical resection, lesion resection were performed in 31 patients and surgical specimens were analysed.
Results Prenatal US and MDCT correctly diagnosed 76.9 and 94 % of the lesions, respectively. Disagreement occurred in six lesions with prenatal US and in two lesions with MDCT. No statistically significant differences were observed between the two techniques ($P = 0.122$).
Conclusions As most surgeons consider the surgical resection of these lesions mandatory, our study underscores the essential role of imaging, in particular CT, in providing invaluable preoperative information on congenital cystic lung diseases recognised in uterus.

Keywords Multidetector computed tomography · Congenital cystic lung disease · Congenital lung malformation · Prenatal ultrasound

Introduction

The first bud of the respiratory tract appears around the fourth week of gestation and originates from the ventral anterior primitive intestine (respiratory diverticulum). Errors at this stage of development are responsible for congenital lung malformations that can be divided into two groups: (a) dysmorphic lung, namely lung agenesis, aplasia and hypoplasia, (b) "focal" malformations or congenital cystic lung diseases (CCLD), namely congenital pulmonary airway malformation (CPAM), pulmonary sequestration (PS), congenital lobar emphysema (CLE), and

M. P. Bondioni · S. Michelini · G. Di Gaetano · P. Tessitore · R. Maroldi
Department of Medical and Surgical Specialties, Radiological Sciences and Public Health, University of Brescia, Brescia, Italy

M. P. Bondioni (✉)
Department of Radiology, University of Brescia, Piazzale Spedali Civili Brescia, 25100 Brescia, Italy
e-mail: bondioni.pia@tin.it

D. Gatta
Unit of Pneumology, Ospedale di Esine, Brescia, Italy

V. Lougaris
Pediatrics Clinic, Department of Clinical and Experimental Sciences, University of Brescia, Brescia, Italy

N. Palai · M. Signorelli
Prenatal Diagnosis Unit, Department of Obstetrics and Gynecology, University of Brescia, Spedali Civili, Brescia, Italy

L. Mascaro
Medical Physics Department, Azienda Ospedaliera Spedali Civili di Brescia, Brescia, Italy

A. Tironi
Department of Pathology, School of Medicine, University of Brescia, Brescia, Italy

G. Boroni · D. Alberti
Department of Pediatric Surgery, University of Brescia, Brescia, Italy

bronchogenic cyst (BC). These last malformations are the focus of our study [1].

CPAMs make up almost 30–40 % of all congenital lung lesions, and are characterised by an excessive overgrowth of the terminal respiratory bronchioles and lung structures with alveolar growth suppression [2]. Genes such as HOXB5, Fgf7, and platelet-derived growth factor-B (PDGF-B) have been implicated in the pathogenesis of CPAM [3–5]. The first Stocker classification from 1977 [6] has been modified and now includes lesions from type 0 to type IV based on the origin of the malformation [7]. Among these lesions, type I are the most frequent while type III lesions are characterised by worse prognosis. Associated malformations involving other organs may be present. PS is the second most common lesion after CPAM, characterised by a portion of lung parenchyma that does not connect with the tracheobronchial system and is therefore not ventilated whereas a systemic arterial supply is always present [2]. Based on the age of onset, PS may be distinguished in intralobar and extralobar; the latter may be associated with other congenital anomalies [1, 8, 9]. CLE is a structural disorder linked to anomalous cartilage development of the bronchus, resulting in the overinflation of one or more pulmonary lobes. Finally, BC occurs at a very early age and originates from an abnormal budding tracheobronchial tree, followed by its non-branching process [1, 8].

The first imaging approach to detect CCLD disease is prenatal ultrasound (PUS), which is usually performed at 18–22 weeks of gestation and allows screening and definition of foetal lung lesions in the majority of cases [10]. Foetal magnetic resonance imaging is also a valuable tool for prenatal diagnosis of CCLD, but for the time being it is only available in few centres.

After birth, multidetector computed tomography (MDCT) plays a key role in the radiological diagnosis of CCLD in children, confirming type and number of lesions and their characterisation, and allowing a thorough preoperative evaluation [8]. MDCT offers the highest spatial resolution and enhanced diagnostic quality, together with multiplanar reformation, which is very informative for the surgeon [11].

Our study aimed to retrospectively evaluate the diagnostic accuracy of MDCT in 33 patients with CCLD. We also compared MDCT with PUS and with surgical and histological findings (and with histology) to evaluate the diagnostic performance of MDCT in defining the right diagnosis and the best surgical planning.

Materials and methods

Patient population

Our institutional review board approved the review of radiological, surgical, and pathological data for this retrospective study. The requirement for parent informed consent was waived. Imaging evaluation included prenatal US and postnatal MDCT.

From June 2004 to April 2012, 33 children with CCLD were evaluated at the Children's Hospital in Brescia, Italy. Our population included 17 males (51.5 %) and 16 females (48.5 %). Age distributions at diagnostic examination and at surgery are presented as box and whisker plots in Fig. 1. According to Tukey's notation [Tukey, John (1977), Exploratory Data Analysis, Addison–Wesley], reported minimum and maximum values are filtered excluding all the outlier points, i.e. points that are greater than 1.5 times the interquartile range. Median, minimum and maximum age at PUS were 20, 19 and 22 weeks, respectively, with 5 outlier values; at CT evaluation, they were 9, 0 and 26 weeks, respectively, with 2 outliers; at surgery they were 17, 0 and 43 weeks, respectively, with 2 outliers. Seventeen patients (51.5 %) were asymptomatic at birth, the others showed symptoms related to respiratory distress.

Prenatal US

In accordance with the international literature [10, 12], the scheduled morphological routine US examination between week 18 and 22 of gestation and PUS evaluation at the third trimester and between week 32 and 35 of gestation were available for the analysis in 27/33 (81.8 %) patients. In some patients, additional US investigations were performed also in late pregnancy to rule out cardiovascular failure, foetal hydrops or polyhydramnios.

PUS was performed by two expert obstetrician–gynaecologists (N.P., M.S.) with an Acuson US scanner (Siemens Medical Systems, Erlangen, Germany) and a 3.5 MHz convex probe. PUS findings were defined according to the following patterns: (1) homogeneous

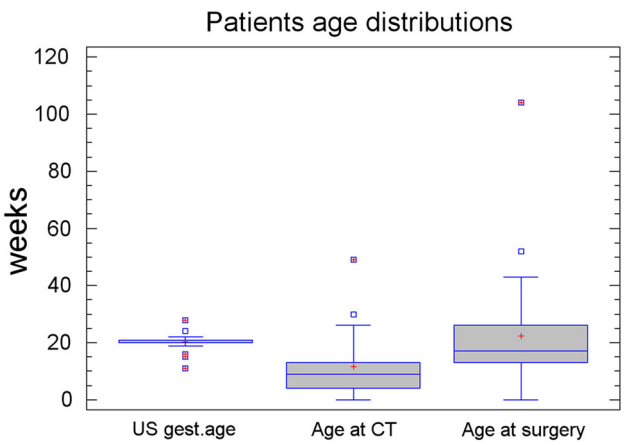

Fig. 1 Patients' age distribution at prenatal ultrasound (PUS), at postnatal multidetector computed tomography (MDCT) and at surgery

hyperechoic lesion (CPAM III); (2) mixed lesion with echogenic component and anechoic component [macrocystic >2 cm (CPAM I) or microcystic <2 cm (CPAM II)]; (3) hyperechoic mass with anomalous arterial supply arising from the aorta (PS); (4) isolated, regular hypoechoic area in the lung (BC).

MDCT

Chest examinations were performed with a 6-slice MDCT scanner (Emotion 6, Siemens Medical Systems, Erlangen, Germany). The area of coverage extended from the thoracic inlet to the diaphragmatic level or just above the renal arteries in the case of a subdiaphragmatic mass detected at PUS. MDCT parameters included 6-mm collimation with age- and weight-based tube current and voltage, high-speed mode, and pitch ranging from 1.0 to 1.5. In all cases, dose modulation was used to minimise the radiation dose.

MDCT was performed after intravenous injection of 2 mL/kg of non-ionic contrast medium (320 mg I/mL). Contrast medium was injected into an antecubital vein with a power injector at a rate of 1.0 mL/s for a 24-gauge catheter, and 1.5–2.0 mL/s for a 22-gauge catheter. Multiplanar (MPR) and 3D reconstructions were acquired for each examination. All patients were sedated.

All examinations were randomly reviewed by two paediatric radiologists (M.P.B., G.D.G.), who were blinded to the prenatal US findings and clinical information. When the reviewers expressed discordant opinions, they reached a consensus by means of a joint review of the recorded images with an additional radiologist (R.M.).

The analysis of the MDCT scans considered the following patterns: (1) homogeneously solid lesion (CPAM III); (2) mixed solid lesion with large cysts >2 cm (CPAM I) or small cysts <2 cm (CPAM II); (3) cystic or solid lesions associated with anomalous systemic arterial supply and venous drainage in intralobar or extralobar PS; (4) hyperinflated lobe with attenuated and displaced vascular structures (CLE); (5) well-circumscribed round or ovoid solitary lesion with uniform fluid attenuation (BC).

Lesion location was assessed according to the standard nomenclature: right upper, middle, lower lobe; left upper, lingula and lower lobe.

Surgery

The thorax was entered through a posterolateral incision, with a muscle sparing technique. Lung lobectomy, segmentectomy, atypical resection or lesion resection were performed when appropriate. All the surgical specimens were sent for histological examination.

Histology

Surgical specimens were sent to the Surgical Pathology Laboratory in buffered formalin 4 % fixative solution. Gross examination was done after fixation. Samples of the specimens were taken for histology, particularly including cysts, nodules and apparently normal lung when recognised, or random when no gross differences were evident. After sample processing and paraffin embedding, slides for microscopy examination were stained with haematoxylin–eosin. Histochemical or immunohistochemical stains were performed when considered appropriate. Histologically specific features related to pulmonary malformations were evaluated: architecture of lung parenchyma, radial alveolar count, cysts, abnormal vessels, lining of cysts, presence of cartilage, goblet cells, muscle cells, sarcomatous component, inflammatory tissue.

Statistical analysis

Summary statistics was performed by means of the Tukey's box–whisker plot, and was carried out with Statgraphic Centurion XV software (StatPoint Technologies, http://www.statgraphic.com). For the comparison of MDCT and PUS frequency of the overall correct and incorrect diagnosis (CPAM, PS and BC), a parametric exact Fisher test was performed using the utilities from the Stanton A. Glanz CD-Rom [13]. The sensitivity and specificity of the two diagnostic approaches in differentiating the pathologies were compared with a Chi-squared test. As histology was considered the gold standard for diagnosis, MDCT and PUS findings were compared with histology. For all tests, the confidence level was set at 0.05.

Results

Prenatal US

Twenty-eight lesions were detected in 27 out of 33 patients for whom PUS was available for the study.

As shown in Table 1, CPAM was diagnosed in 18 patients (66.6 %): four had CPAM type I (22.2 %), 11 CPAM type II (61.1 %), and three CPAM type III (16.6 %). One patient with PS had also CPAM type II in the same affected lung lobe. This CPAM lesion was included in the CPAM statistical analysis for a total of 19 lesions. Lesions showed size changes at the ultrasound follow-up in 10/18 subjects (55.5 %): in particular, in 4/10 cases (40 %) (three CPAM type II and one CPAM type I) the lesions were no longer detectable at the last assessment at 32 weeks of gestation, in 3/10 cases (30 %) (CPAM type

Table 1 US findings during prenatal screening in 27/33 patients

CPAM type I	4
CPAM type II[a]	11
CPAM type III	3
PS[a]	8
BC	1

CPAM congenital pulmonary airway malformation, *PS* pulmonary sequestration, *BC* bronchogenic cyst

[a] One patient with PS and CPAM type II (hybrid lesion)

Table 2 CT findings in 33 patients

CPAM type I[a]	5
CPAM type II[a]	9
CPAM type III	1
Extralobar PS	10
Intralobar PS*	4
CLE	3
BC	1

CLE congenital lobar emphysema

[a] Two patients with intralobar PS had CPAM type I and II (hybrid lesions)

III) the lesions had increased in size and in 3/10 cases (30 %) (CPAM type III) they had decreased in size.

Eight patients (29.6 %) were diagnosed with PS. In 7/8 patients (87.5 %), the diagnosis was easily established; in one case (12.5 %), despite highly suggestive imaging for PS, the diagnosis was only suspected due to the failure to detect an afferent systemic artery.

One patient (3.7 %) was diagnosed with BC.

MDCT

MDCT was performed in all 33 patients (27 with a prenatal diagnosis and 6 symptomatic patients with no prenatal diagnosis). The data are summarised in Table 2.

CPAM was detected in 15 patients (45.4 %). In particular, five had CPAM type I (33.3 %), nine CPAM type II (60 %), and one CPAM type III (6.6 %). Two patients with intralobar PS had also CPAM type I and II, respectively, for a total of 17 lesions.

Lesions were detected in the right lung in ten patients (four CPAMs were located in the right upper lobe, two in the middle lobe, and four in the right lower lobe), and in the left lung in eight patients (two CPAMs were located in the upper lobe, one in the lingula, and five in the lower lobe).

PS was detected in 14 patients (42.4 %): PS was intralobar in 4 patients and extralobar in 10. In two patients, the lesion was found under the left side of the diaphragm. Lesions were located in the left lower thoracic cavity in 50 % of cases (7/14) and in the right lower thoracic cavity in 35.7 % of the cases (5/14); in 14.2 % of the cases (2/14), the lesions were next to the left adrenal gland.

In three patients (9.1 %), the diagnosis was consistent with CLE in the left upper and lower lobe and in the right lower lobe, respectively.

In one patient (3.0 %), the diagnosis was consistent with right BC in the right lower lobe. Lesion location is shown in Table 3.

Table 3 Location of lesions on MDCT in 33 patients

	CPAM (15 pt)	PS (14 pt)	CLE (3 pt)	BC (1 pt)
Left lobe				
Left upper lobe	2/15 (13.3 %)		1/3 (33 %)	
Lingula	1/15 (6.6 %)			
Left lower lobe	5/15 (33.3 %)	7/14 (50 %)	1/3 (33 %)	
Right lobe				
Right upper lobe	4/15 (26.6 %)			
Middle lobe	2/15 (13.3 %)			
Right lower lobe	4/15 (26.6 %)	5/14 (35.7 %)	1/3 (33 %)	1/1 (100 %)
Abdomen (adrenal gland)		2/14 (14.2 %)		

Table 4 Comparison of prenatal US and MDCT findings

	US	MDCT	
Lesions detected	20/26 (76.9 %)	31/33 (94 %)	$P = 0.122$

Surgery

Thirty-one patients underwent surgery. Mean patient age at surgery was 156 days (range, 3 days–24 months). Concerning CPAM, lung lobectomy was performed in five patients, lung segmentectomy was performed in five patients, and atypical resection in three patients. The ten patients with extralobar PS underwent lesion resection, the four patients with intralobar PS underwent atypical pulmonary resection including the sequestration in two cases, and lobectomy in two patients. Patients with CLE underwent lobectomy, and the only patient with BC underwent evacuation by puncture and cystic resection.

No postoperative complications were observed.

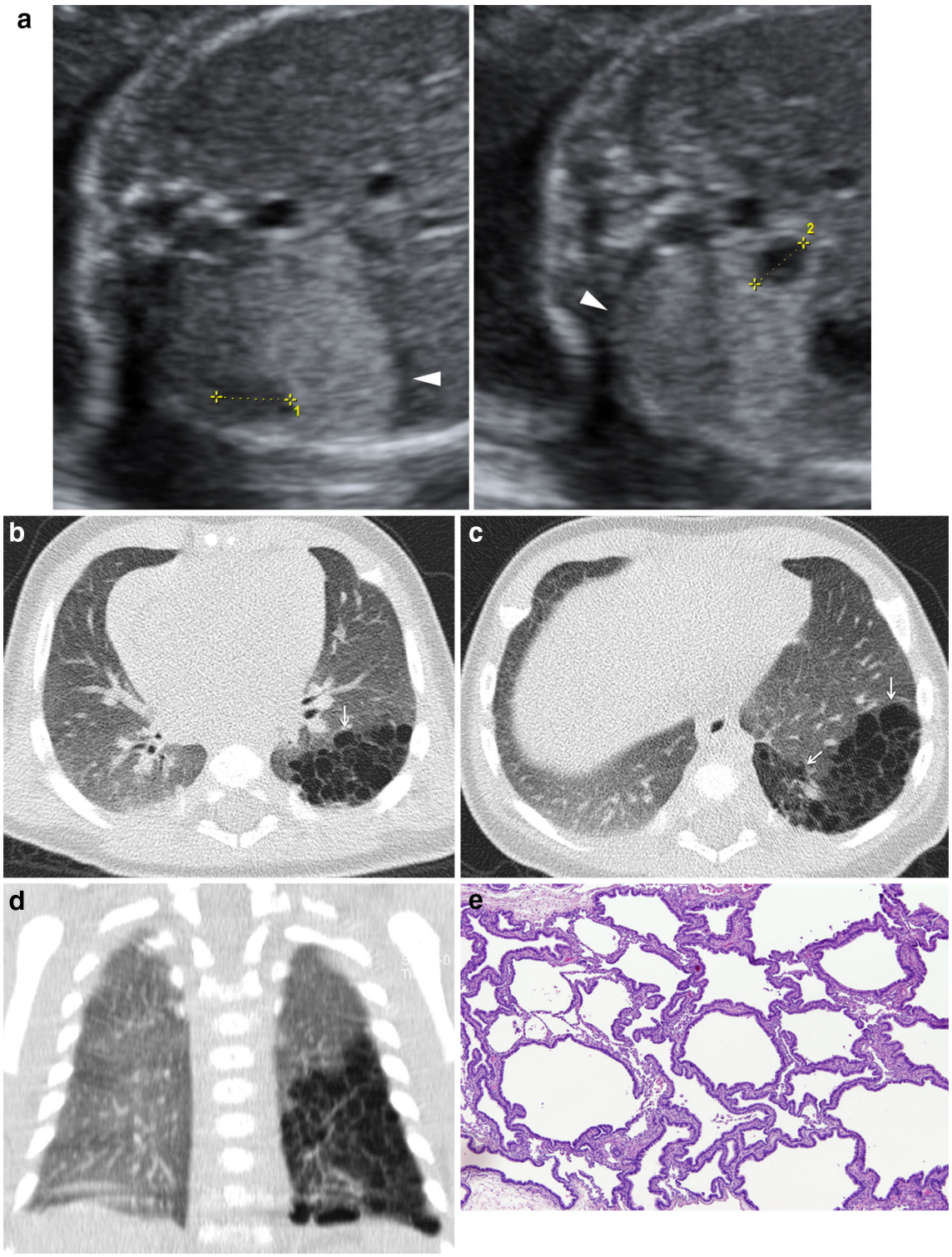

Fig. 2 Patient with congenital pulmonary airway malformation (CPAM) type II. On PUS at 20 weeks of gestation (**a**) a large, hyperechoic lesion (*arrowheads*) with small hypoechoic cystic areas (*clippers*) can be detected. Unenhanced MDCT scans in axial (**b**, **c**) and coronal planes (**d**) show, in the *left lower* lobe, multiple small thin-wall cysts (*arrows*). On microscopic view (e), dilated alveolar spaces lined by normal bronchiolar epithelium can be appreciated (H&E, ×10)

Histology

Histology still remains the gold standard for the diagnostic confirmation of CCLD.

Histological examination of the 33 lesions showed:

- CPAM in 15 cases (45.5 %): five CPAM type I (33.3 %), nine CPAM type II (60 %) (two of them associated with PS–hybrid lesions), and one CPAM type III (6.6 %).
- PS in 14 cases (42.4 %).
- CLE in two cases (6 %).
- BC in one case and inflammatory tissue in one case (3 %).

Comparison between PUS and histological findings

Out of the 27 patients evaluated with PUS, 25 underwent surgery for a total of 26 lesions. PUS was suggestive of the correct diagnosis in 20 out of 26 lesions (76.9 %), 11 CPAM, eight PS, and one BC, as confirmed by histology. Of the two cases of CPAM associated with PS, US correctly identified the two different lesions in only one case, while the other case was diagnosed as PS only. Disagreement occurred in 6 out of 26 lesions (23 %). In particular, one case of CPAM type II was shown to be inflammatory tissue. Four lesions considered to be a CPAM type III were actually PS; one case of CPAM type I was CLE. For CPAM detection, PUS sensitivity and specificity were respectively 100 and 60 %, whilst they were 66.7 and 100 % respectively for PS.

Comparison between MDCT and histological findings

Out of the 33 MDCT patients, 31 underwent surgery for a total of 33 lesions. The comparison between MDCT findings and histology showed a concordance in 94 % of detected lesions (31/33), i.e. 14 CPAM, 14 PS, two CLE, and one BC. Disagreement occurred in 2 out of 33 lesions (6 %): one case of CPAM type II was shown to be inflammatory tissue (possibly due to infection in CPAM). One case diagnosed as CLE was actually CPAM type I. MDCT sensitivity and specificity for CPAM detection were 93.3 % and 93.7 %, while they were both 100 % for PS.

Comparison between PUS findings and MDCT

PUS and MDCT diagnosed correctly 76.9 and 94 % of lesions, respectively. No statistically significant differences were observed between the two techniques (PUS and MDCT), as shown in Table 4 (Fisher exact test, $P = 0.122$).

More in detail, we considered each disorder separately:

- In CPAM, PUS raised the suspicion in 18 patients with 19 lesions, with histological confirmation in 11 out of 17 cases (positive predictive value, PPV = 64.7 %). MDCT raised the suspicion in 15 patients with CPAM and in 2 patients with combined PS and CPAM with a total of 17 lesions with histological confirmation in 14/15 (PPV = 93.3 %). Comparison between the PUS and MDCT findings was not significant for PPV and sensitivity, while it was significant for specificity (Fig. 2a–e).
- In PS, PUS was suggestive in eight patients with eight lesions, and all were confirmed by histology (PPV = 100 %). MDCT was suggestive in 14 patients with 14 lesions, all of which were also confirmed by histology (PPV = 100 %). MDCT sensitivity was significantly different from PUS, while specificity and PPV were the same for both diagnostic examinations and always equal to 100 % (Table 5) (Figs. 3a–f, 4a–h).

Table 5 Comparison of positive predictive value (PPV), sensitivity and specificity for US, CT and histological findings

	US vs. histology	MDCT vs. histology	
PPV CPAM	11/17 64.7 %	14/15 93.3 %	$P = 0.596$
PPV PS	8/8 100 %	14/14 100 %	Not applicable
Specificity CPAM	9/6 (TN/FP) 60.00 % (TN/(TN + FP))	17/1 (TN/FP) 94.44 % (TN/(TN + FP))	0.030
Specificity PS	14/0 (TN/FP) 100 % (TN/(TN + FP))	19/0 (TN/FP) 100 % (TN/(TN + FP))	Not applicable
Sensitivity CPAM	11/0 (TP/FN) 100 % (TP/(TP + FN))	14/1 (TP/FN) 93.3 % (TP/(TP + FN))	$P = 1$
Sensitivity PS	8/4 (TP/FN) 66.66 % (TP/(TP + FN))	14/0 (TP/FN) 100 % (TP/(TP + FN))	$P = 0.033$

TN true negative, *FP* false positive, *FN* false negative, *FP* false positive

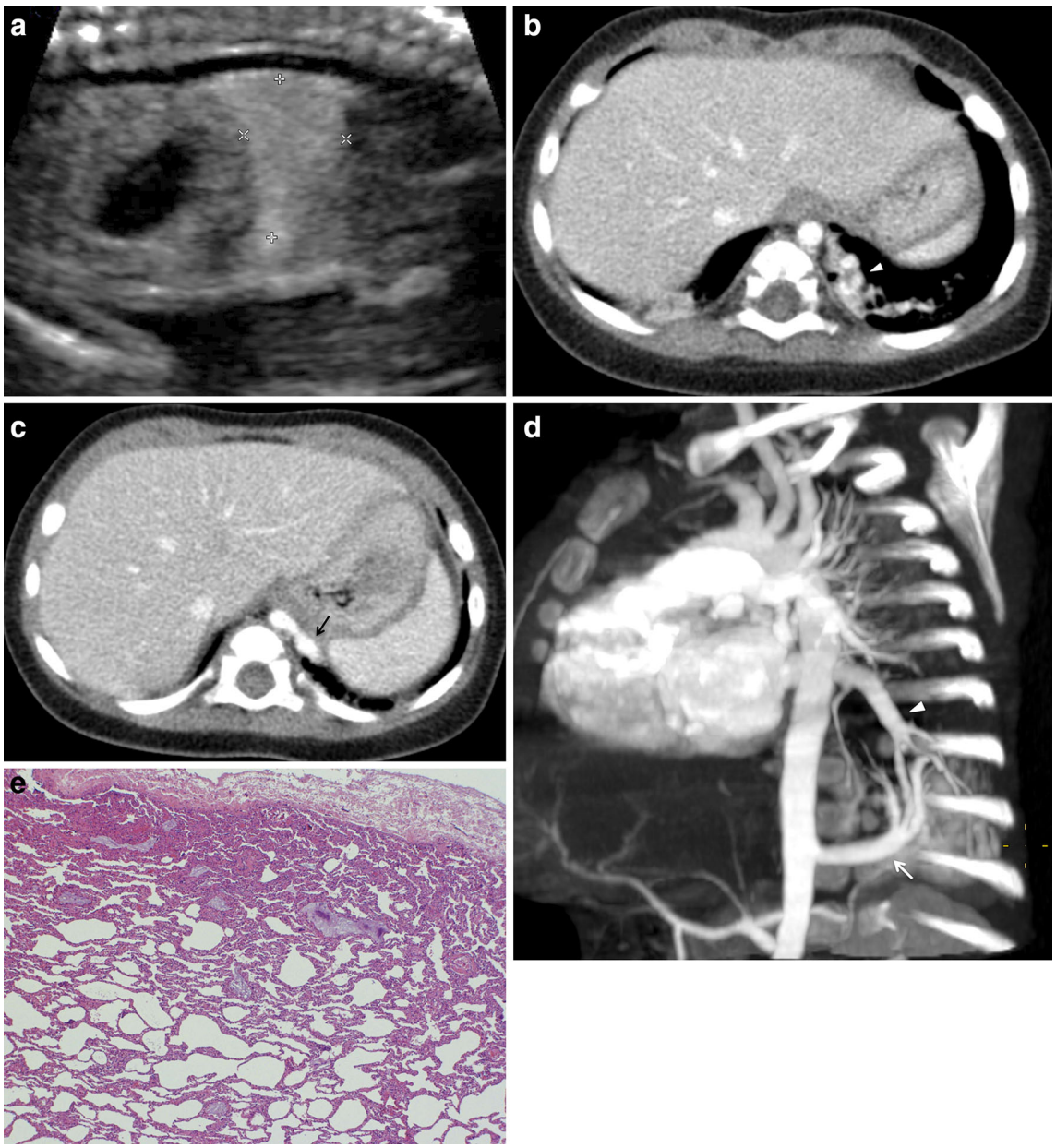

Fig. 3 Patient with intralobar pulmonary sequestration. PUS at 20 weeks of gestation (**a**) shows a homogeneously hyperechoic mass (*clippers*). Postcontrast MDCT scans (**b**, **c**) reveal a hyperdense lesion in the left lower lung (*arrowhead*) with a large artery originating from the aorta (*black arrow*). Maximum intensity projection (MIP) reconstruction (**d**) shows the systemic arterial supply (*white arrow*) and the pulmonary venous drainage (*white arrowhead*). Low power view of intralobar sequestration (**e**) shows pleural fibrosis and mild inflammatory changes in pulmonary parenchyma with mucus in some alveoli (H&E, ×40)

- In the only observed case of BC, both PUS and MDCT diagnoses were confirmed by histology;
- In CLE, only two out of three cases in which MDCT raised a suspicion were histologically confirmed (PPV = 66 %), the remaining case being a CPAM type I. As expected, no diagnosis of CLE was established with PUS.

In 28 out of 31 patients (90.3 %), MDCT was in agreement with surgical findings. In particular, MDCT overestimated the extent of the lesions in three patients with CPAM.

Discussion

Congenital cystic lung diseases include a heterogeneous group of anomalies affecting bronchi, lung parenchyma, arterial supply, and venous drainage. The spectrum of these abnormalities includes CPAM, PS, CLE, and BC [1].

The first diagnostic examination is PUS, usually performed at 18–22 weeks of gestation, during the first scheduled morphological evaluation of the foetus [14]. In

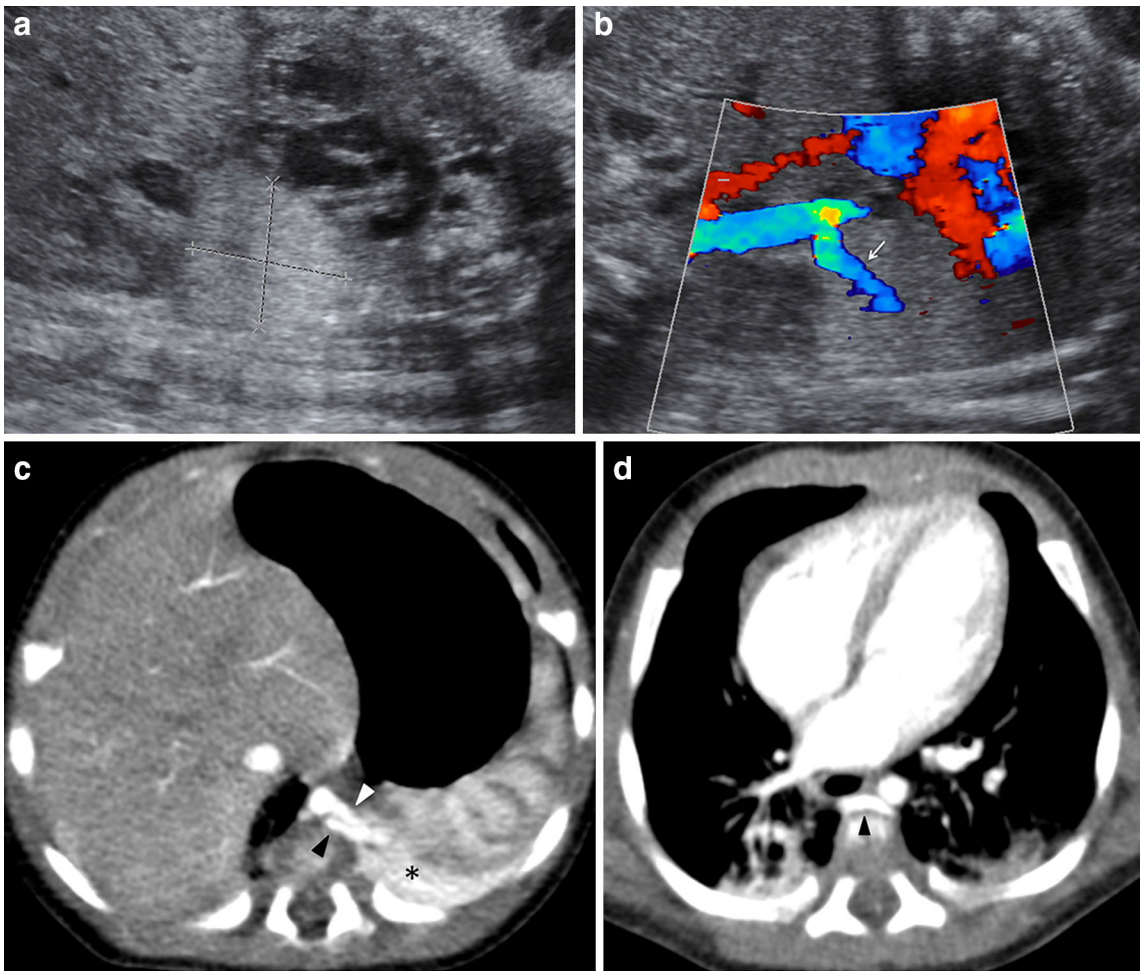

Fig. 4 Patient with extralobar pulmonary sequestration. PUS at 21 weeks of gestation (**a**, **b**), displays a homogenous hyperechoic lesion (*clippers*) with an arterial vessel (*arrow*) entering the mass. MDCT scans after contrast medium administration (**c**, **d**) show a homogeneously hyperdense mass in the left lower lobe (*asterisk*). A feeding artery arising from the aorta (*white arrowhead*) with a venous drainage through the azygous system (*black arrowheads*) can be seen. MIP reconstructions (**e**, **f**) show a marked vascularity of the lesion (*asterisk*), and systemic venous drainage (*white arrows*). On microscopic view (**g**), effaced pulmonary parenchyma with bronchiolar dilatation with mucus, alveolar macrophages and haemorrhage (H&E, ×4)

the literature, the diagnostic accuracy of this method ranges between 56 and 77 %, very similar to our results [10, 15–17].

It has been shown that during pregnancy these lesions may display a variable pattern of growth: they can increase or decrease in size, or even disappear [18]. In our series, lesions increased in size in 30 % of cases, decreased in size in 30 % of cases, and were no longer detectable at the last PUS in 40 % of cases.

After birth, chest X-ray is no longer the first imaging approach, as it fails to detect lesions in about 60 % of asymptomatic patients [19]. However, in clinical practice, chest X-ray is still used as the first-line approach only for patients with respiratory distress. MDCT was performed in all patients with a prenatal diagnosis of CCLD, regardless to its evolution during pregnancy. Our MDCT examinations were performed with age- and weight-based protocol in accordance with the literature, achieving a reduced biological aggressiveness in paediatric patients, particularly in newborn babies and little infants, as were many patients in this study [20–23]. Comparison among PUS and MDCT findings showed a discrepancy with regards to CCLD diagnosis. Specifically, PUS failed to properly diagnose 23 % of cases and MDCT failed in only 6 % of the analysed statistics, as later confirmed by histological examination. However, statistical comparison did not highlight any significant difference between the overall results of the two techniques ($P = 0.122$). This finding underscores the important role of MDCT in the evaluation of CCLD. Furthermore, out of the four patients with no longer detectable lesion at the last PUS, MDCT showed the presence of CPAM in three cases and of PS in one case.

The accuracy of PUS and MDCT diagnosis was then compared with the histological data. To our knowledge,

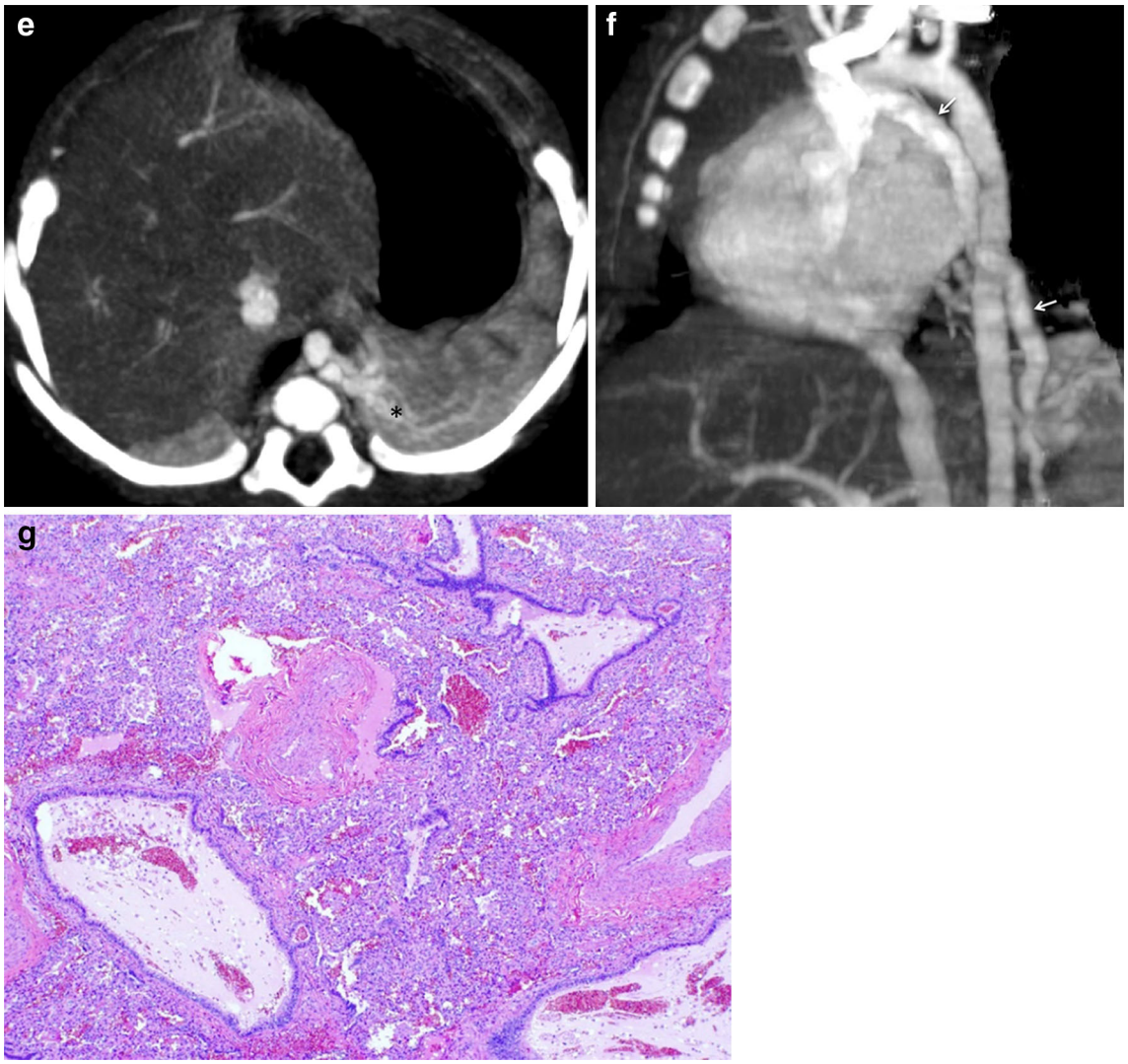

Fig. 4 continued

this study is the first to compare prenatal and postnatal radiological diagnoses with histological findings. Agreement between PUS and histology and MDCT and histology was observed in 76.9 % (20/26) and 94 % (31/33) of the cases, respectively. Overall, the PPV of the survey MDCT scans compared with histology was 93.3 %, compared with a reported value of 70 % in the literature [19]. As most surgeons consider surgical resection of these lesions mandatory, MDCT can provide detailed anatomical localisation of lesions, with the possibility of 3D reconstruction and high spatial resolution. Postprocessing reconstruction can also provide detailed information on vascular afferents, and 3D reconstructions in our study proved to be very helpful to the surgeon during preoperative planning [24, 25]. Providing a correct diagnosis is of utmost importance not only for symptomatic patients, for whom surgery is mandatory, but also for asymptomatic ones. In this subset of patients, the nature of the lesion (e.g. some CPAMs display a potential for malignant transformation) can prompt a surgical operation even in the presence of small lesions. The analysis of our data shows that MDCT should be used as first-step imaging in the postnatal evaluation of patients with CCLD, and our work suggests that MDCT can be considered the best imaging modality in the postnatal evaluation of patients with CCLD detected in uterus, with higher specificity values for CPAM lesions and higher sensitivity for PS compared to PUS findings. Moreover, MDCT gives high spatial resolution, enhanced quality and multiplanar image reformation with detailed information on vascular afferents. As demonstrated by our results, this is a very useful tool to define the surgical approach, since the comparison between MDCT and surgical findings demonstrates a total agreement in 90.3 % of cases.

Furthermore, preoperative MDCT evaluation is highly predictive of the possibility of a "not challenging" minimally invasive surgery (i.e. thoracoscopic resection) in patients with small and peripheral intralobar lesions or extralobar lesions (PS, BC). Thoracoscopic resection in this subset of lesions allows for more rapid and less painful healing with a better cosmetic result, and it prevents any negative effects of the thoracotomy on the patient's growth. Since thoracoscopic pulmonary lobe resection is a highly demanding and potentially dangerous procedure, especially in infants, it must only be performed by expert thoracic paediatric surgeons.

In conclusion, postnatal MDCT can provide invaluable preoperative information on CCLD recognised in uterus.

Conflict of interest Maria Pia Bondioni, Diego Gatta, Vassilios Lougaris, Nicoletta Palai, Marino Signorelli, Silvia Michelini, Giuseppe Di Gaetano, Paola Tessitore, Lorella Mascaro, Andrea Tironi, Giovanni Boroni, Roberto Maroldi, Daniele Alberti declare no conflict of interest.

References

1. Biyyam DR, Chapman T, Ferguson MR et al (2010) Congenital lung abnormalities: embryologic features, prenatal diagnosis, and postnatal radiologic-pathologic correlation. Radiographics 30:1721–1738
2. Gupta K, Das A, Menon P et al (2012) Revisiting the histopathologic spectrum of congenital pulmonary developmental disorders. Fetal Pediatr Pathol 31:74–86
3. Wang X, Wolgemuth DJ, Baxi LV (2011) Overexpression of HOXB5, cyclin D1 and PCNA in congenital cystic adenomatoid malformation. Fetal Diagn Ther 29:315–320
4. Jancelewicz T, Nobuhara K, Hawgood S (2008) Laser microdissection allows detection of abnormal gene expression in cystic adenomatoid malformation of the lung. J Pediatr Surg 43:1044–1051
5. Liechty KW, Crombleholme TM, Quinn TM et al (1999) Elevated platelet-derived growth factor-B in congenital cystic adenomatoid malformation requiring fetal resection. J Pediatr Surg 34:805–809
6. Stocker JT, Madewell JE, Drake RM (1977) Congenital cyastic adenomatoid malformation of the lung. Classification and morphologic spectrum. Human Pathol 8:155–171
7. Stocker JT (1994) Pulmonary pathology. Congenital and developmental diseases, 2nd edn. In: Dail HD, Hemmer SP (eds) Springer, Berlin, p 182
8. Lee EY, Boiselle PM, Robert H et al (2008) Multidetector CT evaluation of congenital lung anomalies. Radiology 247:632–648
9. Stocker JT (1986) Sequestration of the lung. Semin Diagn Pathol 3:106–121
10. Epelman M, Kreiger PA, Servaes S et al (2010) Current imaging of prenatally diagnosed congenital lung lesions. Semin Ultrasound CT MR 31:141–157
11. Lee EY, Tracy DA, Mahmood SA et al (2011) Preoperative MDCT evaluation of congenital lung anomalies in children: comparison of axial, multiplanar, and 3D images. AJR Am J Roentgenol 196:1040–1046
12. Chen HW, Hsu WM, Lu FL et al (2010) Management of congenital cystic adenomatoid malformation and bronchopulmonary sequestration in newborns. Pediatr Neonatol 51:172–177
13. Glantz SA (2007) Primer of biostatistics, 6th edn. McGraw-Hill, New York
14. Sturla HE, Harm-Gerd KB, Tegnander E (2004) Fetal medicine—a reality thanks to ultrasound. Clin Physiol Funct Imaging 24:164–168
15. Williams HJ, Johnson KJ (2002) Imaging of congenital cystic lung lesions. Paediatr Respir Rev 3:120–127
16. Bhide A, Murphy D, Thilaganathan B, Carvalho JS (2010) Prenatal findings and differential diagnosis of scimitar syndrome and pulmonary sequestration. Ultrasound Obstet Gynecol 35:398–404
17. Laje P, Liechty KW (2008) Postnatal management and outcome of prenatally diagnosed lung lesions. Prenat Diagn 28:612–618
18. Winters WD, Effmann EL (2001) Congenital masses of the lung: prenatal and postnatal imaging evaluation. J Thorac Imaging 16:196–206
19. Lanza C, Bolli V, Galeazzi V et al (2007) Cystic adenomatoid malformation in children: CT-histopathological correlation. Radiol Med 112:612–619
20. Siegel MJ, Ramirez-Giraldo JC, Hildebolt C et al (2013) Automated low-kilovoltage selection in pediatric computed tomography angiography: phantom study evaluating effects on radiation dose and image quality. Invest Radiol 48:584–589
21. Aberle DR, Adams AM, Berg CD et al (2011) Reduced lung-cancer mortality with low-dose computed tomographic screening. National Lung Screening Trial Research Team. N Engl J Med 365:395–409
22. de Jong PA, Owens CM (2012) Radiation dose for pediatric patients with cystic fibrosis: a continuous adjustment process and remaining concern. Chest 142:1077
23. Young C, Xie C, Owens CM (2012) Paediatric multi-detector row chest CT: what you really need to know. Insights Imaging 3:229–246
24. Siegel MJ (2005) Pediatric CT angiography. Eur Radiol 15(Suppl 4):D32–D36
25. Frush DP, Herlong JR (2005) Pediatric thoracic CT angiography. Pediatr Radiol 35:11–25